

# Topological Identification of Agent Status in Information Contagions: Application to Financial Markets

Anubha Goel<sup>1,\*</sup>, Henri Hansen<sup>1</sup>, and Juho Kanninen<sup>1</sup>

<sup>1</sup>Computing Science/Financial Computing and Data Analytics Group, Tampere University, Tampere, 33720, Finland

\*anubha.goel@tuni.fi

+these authors contributed equally to this work

## ABSTRACT

Cascade models serve as effective tools for understanding the propagation of information and diseases within social networks. Nevertheless, their applicability becomes constrained when the states of the agents (nodes) are hidden and can only be inferred through indirect observations or symptoms. This study proposes a Mapper-based strategy to infer the status of agents within a hidden information cascade model using expert knowledge. To verify and demonstrate the method we identify agents who are likely to take advantage of information obtained from an inside information network. We do this using data on insider networks and stock market transactions. Recognizing the sensitive nature of allegations of insider trading, we design a conservative approach to minimize false positives, ensuring that innocent agents are not wrongfully implicated. The Mapper-based results systematically outperform other methods, such as clustering and unsupervised anomaly detection, on synthetic data. We also apply the method to empirical data and verify the results using a statistical validation method based on persistence homology. Our findings highlight that the proposed Mapper-based technique successfully identifies a subpopulation of opportunistic agents within the information cascades. The adaptability of this method to diverse data types and sizes is demonstrated, with potential for tailoring for specific applications.

## Introduction

Information contagions occur when individuals, referred to here as *agents*, receive information from their neighbors in a social network. These individuals then spread the information further, resulting in a cascade. Although information contagions can occur in various domains, they are particularly significant in financial markets, where investors seek to leverage private information. For example, insider information about a company spreads within a social network before official release. Those who receive insider information early may trade profitably before the expected market movement. While these trades are not necessarily public and may not be immediately noticed by other investors, individuals with insider information may spread through contacts within a social network. This may result in a cascading effect where the initial information propagates through the network. This influences a group of agents to trade similarly, amplifying market impact before the official announcement.

Several methods of inference have been suggested for analysis of information contagion, such as belief propagation and dynamic message-passing algorithms. These methods usually assume that status of the agents, that is, whether they have received and reacted to the information, is known and observable<sup>1-5</sup>. In practice, the activation status in contagions is often not directly observable. For example, during the COVID-19 pandemic, infection chains and the actual infection statuses of individuals were frequently hidden due to asymptomatic cases, false-positive symptoms, and inaccuracies in rapid antigen tests<sup>6</sup>.

In the scenario of this paper, agents can receive insider information through their social connections, but market supervisors can rarely observe who is informed and who is not. For such cases, we need inference based on indirect evidence, such as agents' actions in stock markets.

Detecting agents whose behavior is influenced by private information obtained through social contacts, rather than by other factors, is a challenging task. For example, in the context of investors with insider information, it might be suspicious if an investor makes profitable trades just before public announcements by a particular company. However, an agent might behave as if they were informed for other reasons, or even randomly. Methodologically, standard statistical and machine learning methods struggle when no ground truth about true activation status is known and there are limited observations for each agent. The data may be sparse and multidimensional, and conventional unsupervised clustering methods are not necessarily effective.

In this paper, we propose a method based on Topological Data Analysis (TDA), specifically the Mapper Algorithm, to address this problem. Our approach is based on detecting clusters and interesting topological structures that traditional methods

often fail to identify. It extracts simple descriptions of original data in the form of simplicial complexes. The main advantage of Mapper is that it works as a soft clustering technique which makes use of expert knowledge to form filter functions, which are then used in data projection.

We apply the method to identify agents whose trading seems to be based on insider information. These agents appear to receive inside information before it becomes public via an announcement. The agents make more profitable trades during pre-announcement periods. The aim is to identify these agents as accurately as possible. We refer to such agents as "opportunistic". Our emphasis is on reducing false positives while still achieving a substantial number of true positive identifications, and demonstrate that the Mapper technique is ideally suited for this purpose.

Because no ground truth about agent status is known empirically, we created a simulation to validate our method before applying it to real world data. The results are reported in the supplementary material.

We then applied the Mapper-based method to empirical trading data from actual investors who are also company insiders. We implement the method to identify opportunistic agents for each company separately, analyzing all investor-company pairs. For  $N$  investors investing across  $M$  companies, this results in  $M \times N$  investor company pairs. The insider network structure is not used in the classification procedure, but it has a strong association with how agents are categorized, providing compelling evidence that differences in trading behavior are mediated by observable social connections. To statistically validate our findings, we utilize the Gibbs distributions for persistence diagrams (GPD) to obtain the distributional forms of persistence diagrams for opportunistic agents identified by the Mapper strategy and compare them to other agents, both in pre-announcement and non-announcement periods. Our analysis reveals statistically significant differences in the distributions of opportunistic agents, and also higher distances between the topological summaries during pre-announcement and announcement periods for these agents compared to others. Another potential approach would involve applying the GPD to all agent-company pairs to detect statistically significant differences in persistence diagrams across the pre-announcement and non-announcement periods, and then identifying opportunistic agents based on profits or other criteria. However, this method is far more computationally demanding. Given the vast amount of data, applying GPD broadly would require impractical computational resources, greatly impacting efficiency without offering substantial additional insights. By focusing on a pre-selected subset of agent-company pairs, our approach balances statistical rigor with computational feasibility, making it both effective and efficient.

## Results

### Our Framework

The idea underlying the Mapper algorithm is to project the complex data in  $\mathcal{X}$  to a much simpler space, usually  $\mathbb{R}^d$ , in a tractable manner through a map  $f$  known as filter function, which projects the high-dimensional data into a lower-dimensional space. The filter functions are formed with *expert knowledge* to capture relevant features for clustering. This is followed by applying topological tools to cover the projection via open sets and finally examining the pre-images of these sets under the filter map. A clustering technique, such as K-means, is applied to each of the pre-images. These clusters are then connected based on how much the open sets overlap. Thus we obtain a graph where nodes represent clusters and connections between nodes represent shared elements.<sup>7,8</sup> The whole procedure returns a simplified version of the original data, retaining its topological properties such as connectedness, 1-dimensional holes, etc. The network then gives rise to a simple visualization of the original data, which is easier to comprehend.

As a clustering algorithm Mapper considers both the local (subgroups of similar data) and global aspects of data points, to create overlapping clusters called soft clusters. This has been shown to improve performance in various data analysis tasks, such as training classifiers<sup>9</sup>.

The primary goal of this paper is to systematically identify a subpopulation of agents, denoted  $\mathcal{Q}$ , who exhibit symptoms that indicate they have received, and acted upon, inside information. A detailed explanation of the method is available in the Methods section located near the end of the paper.

### Application to the Use of Insider Information in Stock Markets

The focus of our research is financial markets, where we have no direct observations of whether agents have received information through their social connections. We hypothesize that before a company makes an announcement, the information is obtained by agents who have access to this inside information. These agents may then spread the information through their social networks. While we have no direct observations on the individual agent statuses in the network, the observations of trading events are considered as possible symptoms of having obtained the information. We consider two criteria: whether an agent is consistently observed making profitable trades just before public announcements, and whether trading performance significantly declines in periods with no upcoming announcements.

In the existing literature, the question of identifying informed investors is rarely addressed, possibly due to a lack of data and reliable methods. One example is Ref. 10, which employs Graph Neural Networks to forecast investors' trading behavior based on trading events within their local social networks. However, they do not incorporate data on information events such as

announcements, and focus solely on the predictability of individuals' transactions within a social network. This approach only indirectly provides evidence that private information is being utilized. There is an expanding body of research on so-called investor networks, which aims at identifying information links between investors, by detecting pairs with significantly high synchronization in their trading behavior<sup>11-14</sup>. Contrary to our research, this field of study focuses on identifying or predicting effective links between investors rather than pinpointing the most opportunistic traders based on their trading behavior. One relevant study is Ref. 15, which analyzes a small hand-collected legal document on both inside traders and people who shared information but did not trade securities themselves. The study discovers that inside information typically originates from corporate executives and that people who trade on this inside information see substantial returns of approximately 35% over a 21-day period. Unlike in Ref. 15, in which direct observations of information arrival were used to discover and analyze who does or does not receive information, our objective is to identify whether an investor traded using private information.

We refer to the agents who trade using inside information as "opportunistic agents". To capture the intuition of what makes an agent opportunistic, we define two filter functions to extract the relevant features of the agents' trading behavior. The first filter function is defined as the number of profitable trades made in the pre-announcement periods, and we denote it as  $F_1$ .

This filter function is necessary but not sufficient for identifying opportunistic agents. For instance, it gives a high score for agents who trade without any information and just happen to trade very often. We thus need to take into account agent-specific abnormal returns. Abnormal returns observed during the information event period, serve as the basis of  $F_2$ . This function maps each agent to the difference between their average daily realised returns in the pre-announcement periods and returns in the non-announcement periods. This criterion was identified, e.g., in<sup>16-18</sup>. Our hypothesis is that an opportunistic agent not only makes several profitable transactions before public announcements but also, their transactions during the pre-announcement periods are on average more profitable than otherwise.

One could implement additional filtering functions, for example, using observations of the social graph of the agents. For example, checking if the agent in question is connected to the insiders of a company they are trading in. However, we chose to leave the social observations out of the classifying procedure. Instead, we use them to validate our method further. We do this by examining the hypothesis that compared to passive agents, the agents classified as opportunistic, are more likely to be indirectly or directly socially connected to insiders and therefore more likely to receive insider information.

To validate the approach against a reasonable model of information contagion, we conducted monte carlo experiments a cascade model was simulated on an actual insider graph. We compared our method with hard clustering and anomaly detection methods. The results showed that our method had superior accuracy. Results are in the supplementary material.

## Empirical findings on insider network

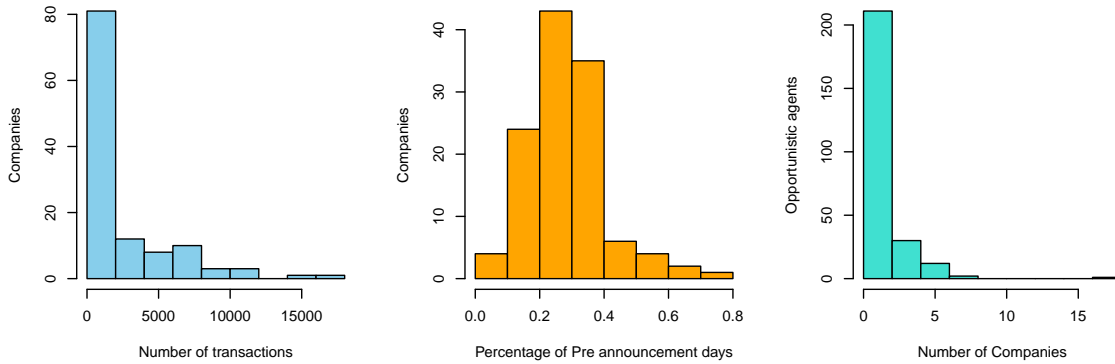
The kernel densities for both opportunistic agents and other agents as identified using the filter functions  $F_1$  and  $F_2$  (Eqs. 1 and 2) are presented in Figure 1(b). The pattern is clear: during the pre-announcement period, opportunistic agents show a large number of profitable trades. These agents also exhibit higher realised returns in the pre-announcement period compared to non-announcement periods, as indicated by the right-skewed plot of filter function 2. For agents not classified as opportunistic, the values of  $F_1$  and  $F_2$  cluster around zero. This suggests a concentration of values near zero for agents that are not classified as opportunistic, contrasting with the dispersed and skewed distributions observed for agents classified as opportunistic, during the pre-announcement period.

The KDE curves confirm that the agents classified as opportunistic are not simply extreme or outlier values in either filter function. The distributions for these agents are broader and more varied, rather than concentrated at the high ends of the scale. Specifically, the wider spread in both  $F_1$  and  $F_2$  indicates that these traders are characterized by a consistent pattern of profitability and abnormal realised returns during pre-announcement periods, but not exclusively due to having the highest values. The method captures a range of behaviors associated with opportunism, rather than just picking up outliers. This suggest that the Mapper method identifies agents whose overall patterns across both profitability and timing of transactions indicate informed and deliberate trading actions.

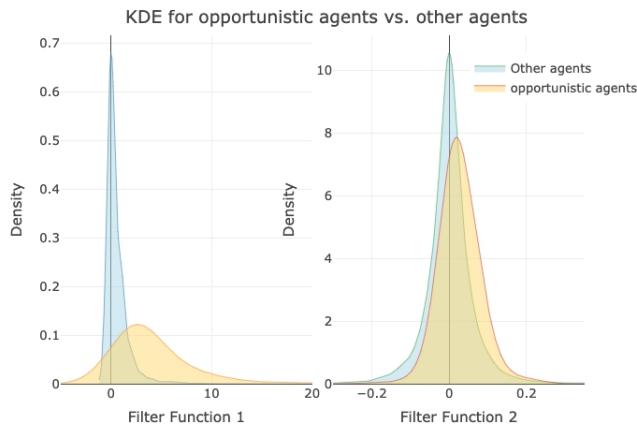
The rightmost plot in Figure 1(a) shows the distribution of agents classified as opportunistic, in terms of how many companies they traded opportunistically on. Only a handful of agents behaved opportunistically with respect to more than just a few companies. Therefore, the opportunistic behavior appears to be very company-specific. This is reasonable, because presumably, very few investors have access to insider information on multiple companies.

A visualisation of the insider network, highlighting agents classified as opportunistic in red, is shown in Figure 1(c). The opportunistic agents are primarily located in the giant component, but they are scattered around the network. This suggests that agents who share private information without taking advantage of it themselves may play a crucial role in spreading information across the network. Assuming opportunistic behaviour is correctly identified by the method, it may also point to the existence of social connections not captured by our data, i.e., social connections that are not based on employment.

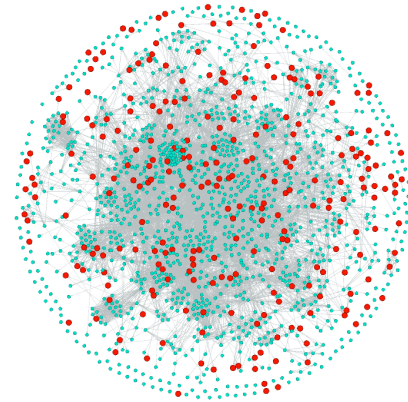
The empirical findings of the Mapper method are summarised in Table 1, including key statistics including profits per agent during both the announcement and non-announcement periods for agents who were classified as opportunistic. Their



(a) Histograms



(b) Kernel Density Plots.



(c) Network Visualization.

**Figure 1. (a) The set of histogram plots** Read from left to right: (1) Number of transactions per company. (2) Percentage of pre-days of companies with respect to the total number of transactions executed by all the investors. (2) The third plot depicts the distribution of companies with respect to the percentage of days within the pre-announcement periods out of all the trading days. (3) The histogram illustrates the distribution of opportunistic traders, showing the number who traded one company opportunistically, those who traded two companies opportunistically, and so on. **(b) Kernel Density Plots:** Comparison of Filter function densities for opportunistic traders and other investors.  $F_1$  represents the number of profitable trades during the pre-announcement period, while  $F_2$  measures the difference in realised returns between the announcement and non-announcement periods. The plots provide a visual overview of the distributions, offering insights into the trading behavior of both opportunistic traders and other investors in response to information received. **(c) Network visualization** where nodes are the investors with edges as links between them. The opportunistic traders as identified by the Mapper strategy are highlighted in red and the others are turquoise colored.

performance is compared with that of the remaining agents. Altogether, 1,586 investors, 119 companies, and 15,668 investor-company pairs (a pair occurs if a specific investor trades a specific stock) were present in our analysis. To control for the effect of liquidity, we filtered the companies based on the number of total transactions, using thresholds of 5,000, 6,000, and 7,000 transactions. This resulted in 24, 18, and 11 companies; 1,215, 1,179, and 1,112 investors; and 8,311, 7,169, and 3,532 investor-company pairs, respectively.

In the data for all 119 companies and 1,586 investors as agents in the network, a subset of 256 (16.14%) agents were classified as opportunistic. When we applied the method to the most liquid companies, the proportion of opportunistic agents decreased. About half of the agents classified as opportunistic were classified based on trading with less liquid stocks. When we analyzed whether agents are connected through the insider network to a company they trade in, we found that using all the data,

among the 454 identified opportunistic agent-company pairs, 342 pairs (75.3%) were interconnected with a maximum seed distance of 6. Similarly, among the 15,214 non-opportunistic agent-company pairs, 11,090 pairs (72.9%) were interconnected with a maximum seed distance of 8.

This association becomes more clear when less-liquid companies are filtered out. When less-liquid companies are filtered out, there is always a connection between opportunistic agents and the seeds. This can be seen as evidence of actual opportunistic behavior and the importance of our identification process. It can be attributed to the more liquid companies being more central in the insider network. To control for this effect, we analyzed the portion of investors who are connected to the company they trade with no more than four steps, and the outcome remains the same. We consider this a strong result. Although we did not use information about the insider network in our classification, we observed an important pattern: opportunistic agents are far better connected to company insiders than other agents. This suggests that we identify truly opportunistic agents. We can also infer that opportunistic agents are less likely to be connected to insiders of less liquid companies.

Keeping in mind that the first filter function measures the number of an agent's profitable trades made in the pre-announcement periods and that the second filter function measures the difference between their average daily realised returns in the pre-announcement periods, we next analyze the results in terms of related, but not exactly similar measures. Firstly, we observe that compared to other agents, agents classified as opportunistic concentrate their transactions, in terms of euro volume, on pre-announcement periods. This is a particularly strong result when data on all companies is used, but the difference also persists across robustness checks when less liquid companies are filtered out. Secondly, we observe that for agents classified as opportunistic 38% of profitable transactions and 24% of unprofitable transactions were executed within the pre-announcement periods, while the percentage is a flat 28% for the other agents. This indicates that opportunistic agents execute a relatively high number of profitable trades and a low number of unprofitable trades before public announcement arrivals. This is a robust result with respect to different data filtering thresholds. Thirdly, when it comes to the euro profits, agents classified as opportunistic generate significantly higher euro profits during pre-announcement times, especially in the most liquid companies (e.g., 22,322 euros in the top 24 companies). This highlights the ability to exploit informational advantages before public announcements. By contrast, opportunistic agents generate negative or minimal profits during non-announcement periods, especially in the most liquid companies (e.g., -3,005.4 euros in the top 24 companies). This suggests that profitability is highly concentrated around informational events, suggesting a reliance on pre-announcement trading strategies rather than sustained performance across all periods. The significant disparity in average euro profit between pre- and non-announcement periods (e.g., 25,327.4 euros in the top 24 companies) is suggestive of opportunistic agent's reliance on exploiting information asymmetry. This further indicates that we were successful in identifying agents who are not merely participating in the market but are systematically exploiting specific periods.

Although opportunistic agents maintain full connectivity in the most liquid companies, their influence in terms of euro volume during pre-announcement periods diminishes sharply from 65% in the top 24 companies to 25% in the top 11 most traded companies. This suggests that heightened regulatory scrutiny and market surveillance in these highly liquid companies reduce the ability of opportunistic agents to exploit informational advantages.

In Ref. 10, investors' trading decisions for the next day were predicted based on how their social neighbors traded today, using Graph Neural Networks. The goal was to identify investors whose trading decisions are influenced by their social connections. Investors whose decisions were highly predictable based on information from the social graph were considered to be behaving suspiciously. They used almost the same data, and an interesting question is whether these two completely different approaches yield overlapping results. Our current research shares 27 of these companies, for which there were 1,284 investors in total. Out of them, we classify 125 agents as opportunistic, while 158 were identified to behave suspiciously in Ref. 10, with an overlap of 50 investors. Using Fisher's Exact Test (based on the hypergeometric cumulative distribution), the p-value for the overlap is less than  $10^{-10}$ , indicating an extremely strong statistical significance. This means that such overlap cannot be explained by randomness. This shows a considerable alignment between the two completely different approaches, which further verifies both the methods presented in this paper and in Ref. 10.

We additionally ran DBSCAN clustering on the empirical data, as it yielded the second-best results in the simulated data scenario, following the Mapper strategy. DBSCAN identified 951 agents as opportunistic out of a total of 1,284, with an overlap of 112 traders with the 125 opportunistic traders identified by the Mapper algorithm and an overlap of 130 traders with the 158 suspiciously behaving investors identified in 10. Notably, the overlap between DBSCAN and other methods is higher not due to superior accuracy, but rather because DBSCAN tends to classify a larger number of traders as opportunistic traders, indicating a higher error rate. This divergence suggests that DBSCAN's clustering results are less precise compared to the Mapper algorithm, as the method appears to be overestimating the number of opportunistic traders. This aligns strongly with the observation made with the simulated data.

	All data	Data for 24 most traded companies		Data for 18 most traded companies		Data for 11 most traded companies		
Companies	119	24		18		11		
Number of investors	1,586	1,217		1,179		1,112		
Number of investor-company pairs	15,668	8,311		7,169		4,532		
Minimum number of transactions	59	5,000		6,000		7,000		
	Opportunistic	Others	Opportunistic	Others	Opportunistic	Others	Opportunistic	Others
Investors	256 (16.14%)	1,330 (83.86%)	126 (10.35%)	1,091 (89.65%)	123 (10.43%)	1,056 (89.57%)	47 (4.23%)	1,065 (95.77%)
Percentage of connected investor-company pairs	75.3%	72.9%	100%	77.6%	100%	77%	100%	77%
Percentage of connected investor-company pairs within 4 steps	71.4%	70.6%	77.66%	74.7%	78.4%	75.16%	81.8%	75.16%
Fraction of euro volume in pre-announcement periods	57%	51%	65%	60%	27%	26%	25%	23%
Fraction of profitable transactions in pre-announcement periods vs all profitable transactions	38%	28%	39%	31%	38%	31%	33%	29%
Fraction of unprofitable transactions in pre-announcement periods vs all unprofitable transactions	24%	28%	26%	31%	26%	31%	21%	30%
Euro profit in pre-announcement periods per investor	11,991.5	-2,461.0	22,322.0	-1,455.6	933.6	92.0	920.8	164.8
Euro profit in non-announcement periods per investor	94.8	3,079.7	-3,005.4	3,963.6	-1,072.3	322.1	-2,847.7	340.4
Difference of Average Euro profit pre and non-announcement periods per investor	11,896.7	-5,540.7	25,327.4	-5,419.2	2,005.9	-230.1	3,768.5	-175.6

**Table 1.** Performance Metrics Comparison between opportunistic and other agents. The table presents results for different cases of analysis. The first column contains the whole data, and from left to right, we filter out companies with fewer than 5,000, 6,000, and 7,000 transactions respectively. The percentage of connected investor-company pairs reports the proportion of pairs where an investor is directly or indirectly connected to a company they traded in, in the insider network.

## Statistical validation using the topology of the data

### Persistence diagrams

Statistical validation is crucial to ensure the reliability of the results. The sparse nature of our data makes it challenging to use conventional distribution models. To address this issue, we employ TDA to establish the statistical validity of our findings by examining the topological characteristics of the data. Our specific aim is to answer, whether the topological properties of investor transactions between pre-announcement and non-announcement periods differ more for the agents that were identified as opportunistic by Mapper compared to other agents. The intuition behind this is that opportunistic agents are more probable to alter their trading behavior when new information is about to be released, and that this would be facilitated by their access to inside information through their social connections.

TDA involves the study of point cloud data, which consists of a set of data points in a given coordinate system with a defined distance or similarity measure. By examining the structural properties of this data, such as connectivity and shape, TDA provides a way to analyze the geometric and topological characteristics of the data beyond mere numerical values. One key tool in TDA is homology, an algebraic method for examining the topological features of a data space. Homology identifies  $k$ -dimensional holes, specifically  $k = 0$  corresponds to connected components,  $k = 1$  to loops, and  $k = 2$  to voids. Persistent homology builds on this by illustrating how these topological features evolve over different scales. Specifically, we apply this method to analyze the super-level sets of real-valued functions  $g$  defined over a space  $Z$ , denoted as  $Z_\alpha = \{z \in Z : g(z) \geq \alpha\}$ .

The  $k$ -th homology group  $H_k$ , for  $k = 0, \dots, \dim(Z)$ , describes the  $k$ -dimensional holes, and its rank, known as the Betti number  $\beta_k$ , counts the number of these holes. The Betti numbers often serve as a summary of the topology of each  $Z_\alpha$ . Specifically,  $\beta_0$  represents the number of connected components in  $Z_\alpha$ , while, in general,  $\beta_k$  counts the number of  $k$ -dimensional holes in  $Z_\alpha$ . Persistent homology improves this approach by tracking how these homological features persist and change as the parameter  $\alpha$  varies (see Methods for details). This method provides a more dynamic view of the topology, allowing us to observe the birth and death of features across different scales. This gives insights into the multi-scale structure of the data that basic homology alone cannot provide. By taking into account the persistence of topological features, persistent homology captures not just a space's static topological features but also how these properties evolve, providing a more complete knowledge of the underlying form and structure.

Persistent homology is unquestionably the most popular method in the rapidly expanding area of TDA, thanks in large part to its ease of visualization via persistent barcodes and diagrams. In the context of super-level set filtration, each bar in a persistence barcode represents an interval that starts (is ‘born’) at a level  $\alpha = b$ , where a new feature in the homology of  $Z_\alpha$  emerges, and ends (dies) at a lower level  $\alpha = d < b$ , where this feature disappears<sup>1</sup>. Persistence diagrams, which plot the points  $(b, d)$ , give an analogous depiction of barcodes.

The parametric model for a persistence diagram can be obtained by using Gibbs distribution<sup>19</sup> (see Methods for details). We refer to this approach as Gibbs distribution for persistence diagrams (GPD). The primary motivation for using GPD for statistical validation of our findings is attributed to our constrained data scenario, wherein we possess only a single sample of the investor data. GPD is specifically tailored to function effectively with a single persistence diagram, making it a suitable choice for our analysis. In this paper, the goal is to define distributions over the space of persistence diagrams for opportunistic traders during both pre-announcement and non-announcement periods. The aim is to observe statistical differences in these distributions and to apply the same analysis to other types of traders as well.

It is crucial to understand that the GPD method alone cannot definitively identify opportunistic traders. The statistical differences observed between the persistent diagrams during pre-announcement and non-announcement periods do not, by themselves, indicate opportunistic trading behavior. To address this limitation, we apply the GPD method specifically to investor categories identified by the Mapper algorithm. This approach allows us to analyze whether opportunistic traders, as categorized by Mapper, exhibit distinct topological properties in their behavior compared to other types of investors. For instance, consider two investors: one exhibits high trading activity outside the announcement period, while the other intensifies trading before announcements. Both show statistically significant differences between their persistent diagrams in the pre-announcement and non-announcement periods. However, these differences alone do not distinguish between the opportunistic and non-opportunistic trader. The first investor, who trades heavily outside the announcement period, is not opportunistic, whereas the second, who strategically increases activity before announcements, is. This example underscores that statistical significance in persistent diagrams must be interpreted within the context of investor behavior to identify true opportunism.

The first step in analyzing the topology of transaction space is to obtain persistence diagrams using the point cloud of transaction data for the investors in both the pre-announcement period and the non-announcement period. To construct the point cloud, we use two key metrics: daily transaction realised returns and profits. Specifically, the point cloud for the announcement period for an investor  $i$  is represented by the matrix  $X_i = [R_{ij}, P_{ij}]_{j \in A_i}$ . Here,  $P_{ij}$  represents the euro profit from transaction  $j$ , where profit is computed by multiplying the realized return by the transaction volume (in Euros). Persistence diagrams are constructed on the top of these point clouds using super-level set filtration. For illustration purposes, we present the persistence diagrams of randomly selected opportunistic traders during both the announcement and non-announcement periods with barcodes that depict the persistence of the topological features in SI. For completeness and a visual comparison, we plot the same for a randomly selected investor, who is not an opportunistic trader. In addition to comparing the distributions of PDs, we also statistically confirmed that the opportunistic agents have different PDs in pre-announcement and non-announcement periods, and the difference in PDs as measured by Wasserstein distances is significantly greater than the non opportunistic agents (see SI).

### **Parameters of the distributions of persistence diagrams are different between opportunistic and other agents**

We analyze the fitted distributions of persistence diagrams (PDs) from observations during both the pre-announcement and non-announcement periods to identify potential differences in distribution parameters. This process begins with fitting the parametric GPD model, represented by the parameter set  $\Theta = (\theta_1, \theta_2, \dots, \theta_n)$ . A crucial step in this process is determining the optimal number of parameters  $n$ , which we evaluate separately for homology groups  $H_0$  and  $H_1$ . After systematically testing parameter counts from 1 to 4 using goodness-of-fit measures, we determine that the best fit requires 4 parameters for  $H_0$  and 1 parameter for  $H_1$ . Given two PDs with the parameters  $\Theta_i = (\theta_1^i, \theta_2^i, \dots, \theta_n^i)$  for  $i = 1, 2$ , we then assess statistical differences between the distributions using the test statistic  $T$  (see Methods section).

Next, we specifically compared the distribution of PDs for agents classified as opportunistic during both periods. Our analysis revealed significant differences in the distribution of PDs between these periods. Given the identified 4 parameters for  $H_0$  and 1 parameter for  $H_1$ , we applied the Bonferroni correction to account for multiple comparisons. The results of these tests, including minimum p-values derived from the t-test, are shown in Figure 2, highlighting the differences across all parameters for both homology groups. We analyzed 454 opportunistic agent-company pairs identified by our approach, but were able to fit the model to both pre-announcement and non-announcement period transaction data for 291 pairs, as the remaining lacked sufficient points in the persistence diagrams to fit the GPD. The test results reveal that for 244 of these pairs, we obtained p-values below 0.002, signifying statistically significant differences in the persistence diagram distributions between the two periods. Overall, we rejected the null hypothesis at a 90% confidence level for 88% of the investor-company pairs. Notably, for the 24 most traded companies, the null hypothesis was rejected with a 90% confidence level in over 92% of cases.

<sup>1</sup>In this sequel, we consider analyzing the persistent homology for zero-dimensional and one-dimensional features i.e. we take  $k = 0, 1$ .

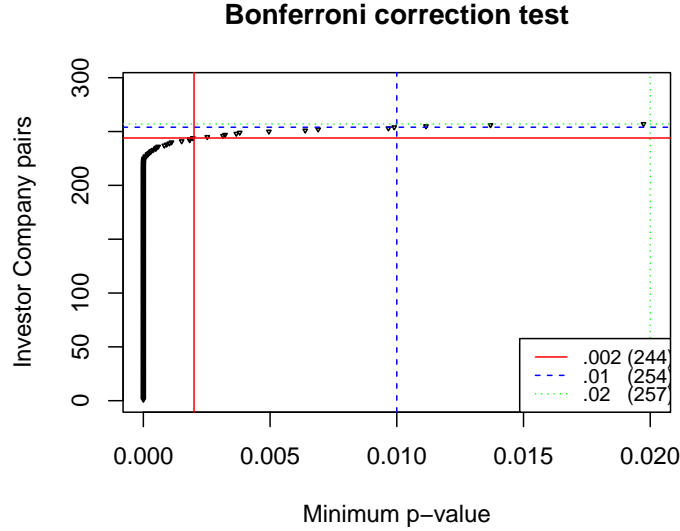


**Figure 2. Minimum p-values with Bonferroni Correction t-Test Results:** The plot displays outcomes from t-tests examining the statistical differences in the distribution of persistence diagrams for opportunistic investor-company pairs during announcement and non-announcement periods. It highlights the minimum p-values across all the distribution model parameters, with horizontal lines indicating the threshold value  $\frac{\alpha}{m}$ . A Green Line Represents  $\alpha = 0.1$ , Blue Line Represents  $\alpha = 0.05$  and a Red Line Represents  $\alpha = 0.01$ , where  $m = 5$  (4 for group  $H_0$  and 1 for group  $H_1$ ). The corresponding lines represent the number of investors falling below the minimum p-value, as indicated in the legend.

We extended our investigation to determine whether the observed differences in the parameter estimates of the distributions for opportunistic agents are larger than those for non-opportunistic agents. For all opportunistic agent-company pairs we constructed a reference set as follows: for each agent-company pair  $(A^s, C_j)$ , where  $A^s$  is the opportunistic agent and  $C_j$  is the corresponding company, we identified a counterpart  $(A^{ns}, C_j)$ , where  $A^{ns}$  is an agent who transacted with  $C_j$  but was not labeled as an opportunistic. Let  $T_s$  (defined in Eq. (3)) represent the test statistic representing the difference in parameters of persistence diagrams for opportunistic agents during announcement and non-announcement periods and  $T_r$  for the non-opportunistic counterparts. To assess whether  $T_s$  is significantly greater than  $T_r$ , we conducted a hypothesis test with the null hypothesis  $H_{null} : T_r \geq T_s$  and the alternative hypothesis  $H_{alt} : T_r < T_s$ . The intuition behind the alternative hypothesis is that opportunistic agents' trading behavior during the pre-announcement and non-announcement periods may differ more compared to non-opportunistic agents (the reference dataset). For robustness, we sampled the reference dataset 30 times and summary stats for p-values for the four parameters associated with homology group  $H_0$  are presented in Table 2. Note that for homology group  $H_1$ , we were unable to draw any conclusions due to the limited number of one-dimensional features in the persistence diagrams. We observe that, across all parameters, the p-values are consistently less than 0.01, signifying substantial differences in the parameter estimates for the opportunistic agents during the pre-announcement and non-announcement periods than the non-opportunistic ones. Although the p-values for  $\theta_0$  are relatively higher in some cases, the p-values for the remaining parameters remain significantly low, as reflected in the maximum p-values across these parameters. This pattern reinforces the conclusion that the observed differences in parameter estimates for opportunistic agents are statistically meaningful and higher than the non-opportunistic agents.

## Discussion

In this study, we introduced a Mapper-based topological data analysis strategy that incorporates expert knowledge to identify opportunistic agents in financial markets. This integration of expert knowledge into the Mapper framework is the key innovation of our approach. The method focuses on relevant features that enhance the accuracy of detecting patterns in the data. While we applied this method to financial markets, its utility extends to any contagion scenario, including the spread of diseases or rumors in networks.

To validate our method, we conducted simulations on synthetic data where the true status of each agent was known. We compared the Mapper strategy with alternative techniques, including K-means, K-means++, DBSCAN, Hierarchical



	$\theta_0$	$\theta_1$	$\theta_2$	$\theta_3$
<b>Min.</b>	2.17E-03	3.82E-21	2.06E-26	1.21E-19
<b>Median</b>	3.39E-03	5.00E-18	5.44E-22	6.09E-16
<b>Mean</b>	5.72E-03	7.35E-11	1.63E-10	1.53E-09
<b>Max.</b>	3.89E-02	1.12E-09	3.92E-09	4.60E-08

**Table 2.** Statistical Analysis of p-Values on  $H_{null} : T_r \geq T_s$ : Evaluation of t-test results to assess whether the difference in parameter estimates of the Persistence Diagram distributions in the pre-announcement vs non-announcement periods for opportunistic traders is greater than that for other investors across all 30 reference datasets. The presented p-value summaries correspond to tests applied to all four parameters associated with group  $H_0$ .

Clustering (Hclust), One-Class Support Vector Machines (OCSVM), K-Nearest Neighbors (KNN), Isolation Forest (IForest), and Local Outlier Factor (LOF). Our approach demonstrated superior performance, particularly in minimizing false positives. A conservative approach is needed in applications such as insider trading detection, where false accusations can carry significant consequences. Our method maintained a high precision across different baseline distributions, whereas other methods struggled with increased false positives as similarity between distributions of behaviours increased.

After validation we applied our strategy to empirical trading data from actual investors and company insiders. By focusing on company-investor pairs, we demonstrated how opportunistic agents are classified without explicitly modeling social connections. The statistical validation of our results using Gibbs distributions for persistence diagrams (GPD) further revealed significant differences in the trading behavior of opportunistic agents during pre-announcement versus other periods.

Our study revealed that opportunistic agents exhibited significantly different trading behaviors as measured from the distributions of their persistence diagrams in the pre-announcement and other periods, along with higher Wasserstein distances between the persistence diagrams during pre-announcement and non-announcement periods compared to the other agents. This finding supports the hypothesis that these agents are influenced by inside information. While computational challenges prevented us from applying the GPD method to all investor-company pairs, our targeted approach proved computationally feasible without sacrificing statistical rigor, making it an effective solution for large datasets.

For broader applicability, the Mapper-based strategy offers potential beyond financial markets. The flexibility of the method makes it suitable for analyzing various types of information cascades, such as the spread of diseases, social influence, or misinformation. The success of the Mapper approach in these contexts depends on defining appropriate domain-specific filter functions that capture the most relevant features of the analysed behaviour. For example, in the case of disease spreading, filter functions could be defined based on transmission rates, geographic location, or individual mobility patterns. In social influence networks, filter functions could be designed to measure the frequency and impact of interactions or the reach of messages. In misinformation networks, filter functions could focus on content virality or user engagement metrics. By tailoring the filter functions to the specific characteristics of the data, Mapper can accurately identify critical agents, whether they are disease super-spreaders, key influencers, or sources of misinformation, making it a valuable tool for when agent status must be inferred from observable behaviors indirectly.

Certain limitations of the approach remain. Applying GPD across all possible pairs would allow deeper analysis, but the computational demand is high. Future research could focus on computational aspects or approximations that maintain accuracy without sacrificing efficiency. Additionally, the use of social network characteristics could enhance precision by directly modeling the flow of information between agents.

In conclusion, the Mapper-based strategy is a significant advancement in the detection of insider trading and a robust tool for identifying hidden patterns in agent behavior. Combining expert knowledge with topological data analysis and persistence homology, it goes beyond conventional techniques, offering an adaptable framework for tackling complex, multidimensional data. It is applicable across a wide range of domains, from tracking disease outbreaks to analyzing social influence and misinformation spread. This positions the Mapper-based strategy as a potentially transformative approach for challenging problems in data science and network analysis.

## Methods

### TDA Mapper

Here we explain how we use the Mapper framework to identify the status of agents based on their trading behaviour. The Mapper algorithm, which is based on generalized Reeb graph<sup>7</sup>, simplifies complex datasets into a one-dimensional graph, making it easier to visualize and analyze data that would otherwise be challenging to study statistically or visually. The stability of Mapper graphs has been discussed in detail in Ref. 20. The Mapper method relies on two main components: a dataset  $X$

with a predefined distance measure  $d$ , and a filter function  $f : X \rightarrow \mathbb{R}$ . The key steps involved in the Mapper algorithm are as follows.

**Lens Function:** First, we project the dataset  $X$  into a lower-dimensional space using a lens or filter function as  $f : X \rightarrow \mathbb{R}^d$ . This step reduces the complexity of the dataset while retaining important information, similar to looking at the data through a special "lens". The lens function is carefully chosen to reflect specific features of interest in the data.

**Level-Set Formation and Covering:** Next, we cover the projected data  $f(X)$  using overlapping sets (called level sets)  $U = \{U_i\}_{i \in I}$  in  $\mathbb{R}^d$  that covers the image of  $X$ , i.e.,  $f(X)$  as  $f(X) \subseteq \cup_{i \in I} U_i$ , where  $I$  is some finite indexing set. It's important to note that this covering groups nearby data points together, regardless of how similar they were in the original  $X$  space.

**Pullback Cover:** We create a Pullback cover by examining the subsets of  $X$  that are lensed into each individual cover set by  $f$ . The pullback cover is the collection of sets in  $X$  and is defined as  $f^{-1}(U_i)_{i \in I}$ . It is worth mentioning that the data points within  $f^{-1}(U_i)$  may not necessarily be globally similar but they correspond to a certain range of the filter function  $f$ .

**Clustering:** For each  $i \in I$ , we employ a clustering algorithm using the distance measure  $d$  to cluster the data points contained within the pre-image  $f^{-1}(U_i)$ . This procedure yields a set of clusters or connected groups, denoted as  $C_{i_1}, C_{i_2}, \dots, C_{i_j}$ . It is worth noting that this clustering process takes place within the original data space,  $X$ . This step enables Mapper to capture similarities in two distinct manners: one within the original data space and the other related to specific properties of interest reflected via the filter function  $f$ .

**Graph Representation:** Finally, we construct a graph, which can be thought of as a simplified network of nodes which consist of the set of all clusters

$$\{C_{i_1}, C_{i_2}, \dots, C_{i_j}; 1 \leq i \leq |I|\}.$$

where an (unoriented) edge between nodes  $C_{j_i}$  and  $C_{k_l}$  is added if and only if  $C_{j_i} \cap C_{k_l} \neq \emptyset$ .

As can be seen, Mapper requires the selection of a filter function and a clustering method, alongside the set of input parameters  $\Gamma = (|I|, p, \theta)$ , where  $|I|$  is the number of level sets, which are of equal size;  $p$  is the percentage of overlap between neighboring level sets; and  $\theta$ , the parameters utilized in the clustering algorithm. It should be emphasized that the choice of clustering algorithm does not impact the performance of Mapper. The pivotal aspect here is the filter selection, which serves as a distinctive lens through which data is examined. Changing the filter leads to different value orders along the filter's range, distinct overlapping intervals, and ultimately results in different sets of clusters, nodes, and features. There is no universal scheme for defining the filter function. Instead, the choice depends on identifying the aspect of the data that is most relevant.

Mapper stands out for its numerous advantages when compared to traditional clustering methods. One key advantage is its ability to seamlessly incorporate prior knowledge by selecting a filter. By choosing specific variables as a lens through which to examine their data, users can effectively direct the clustering algorithm toward theoretically relevant targets. Another benefit of Mapper is its ability to prevent the artificial/hard division of continuous data into distinct clusters. Instead, it forms clusters within overlapping data intervals, preserving the data's inherent continuity. Additionally, Mapper serves as a valuable feature selection tool by encompassing all variables as filters, systematically assessing their capacity to identify and differentiate meaningful subpopulations of interest.

A summarized overview of the procedure is as follows:

1. Define  $n$  filter functions  $f_i$  where each function maps agents to the values corresponding to specific symptom attributes. The  $i$ th filter function specifically maps agents to the value of the  $i$ th attribute.
2. Generate  $n$  Mapper graphs using these filter functions.
3. Set target values for each attribute. This is done by identifying a target bin  $k$  with prominent symptom values.
4. Select clusters  $C_{k_1}, C_{k_2}, \dots, C_{k_j}$  from the  $i$ th Mapper graph, and soft clusters (clusters linked to other clusters) i.e. remove  $C_{k_m}$  if  $C_{k_m} \cap C_{q_l} \neq \emptyset$ , for  $k \neq q$ , resulting in a set  $S_i$  comprising subpopulations within the remaining hard clusters.
5. Take the intersection of the subpopulations  $S_i$  to create the set  $Q = \bigcap_{i=1}^n S_i$ .

This strategy offers both adaptability and repetition. For instance, the strategy can be applied to obtain a subpopulation. This subpopulation then becomes the population set for another application of the same strategy, enabling a high-resolution analysis. This iterative approach allows for a detailed and user-specific exploration of the population without changing the strategy's core framework.

Let  $X_i$  represent the vector containing realised returns for each transaction of the  $i$ th investor for a given company. Assuming there are  $M_i$  transactions, we write  $X_i = (R_{i1}, R_{i2}, \dots, R_{iM_i})$ , where  $R_{ij} \in \mathbb{R}$  for all  $j \in [1, M_i]$  indicates the investors realised returns on the transaction. Then, for investor  $i$ , each transaction is classified as either occurring during the pre-announcement

period or the non-announcement period. When transaction  $j$  occurs within the pre-announcement period, we write  $j \in A_i$ , and otherwise  $j \notin A_i$ . We define the function  $F_1 : X_i \rightarrow \mathbb{Z}$  as follows:

$$F_1(X_i) = \sum_{j \in A_i} \mathbf{1}_{R_{ij} > 0}. \quad (1)$$

We define the function  $F_2 : X_i \rightarrow \mathbb{R}$  as

$$F_2(X_i) = \frac{1}{|A_i|} \sum_{j \in A_i} R_{ij} - \frac{1}{M_i - |A_i|} \sum_{j \notin A_i} R_{ij}. \quad (2)$$

The second filter function is equal to the investor's average return from transactions during the pre-announcement periods, minus the average return from other transactions.

### Persistence diagrams with super-level set filtration

We provide an overview of persistent homology and persistence diagrams constructed using the superlevel-set filtration. For a comprehensive understanding, see Ref. 21 for a more in-depth exploration.

Let  $Z$  be a compact subset of  $\mathbb{R}^D$ . A filtration of  $Z$  is represented as a sequence of increasing subsets:  $Z_1 \subseteq Z_2 \subseteq \dots \subseteq Z_n = Z$ , which provides a systematic way to explore and inspect  $Z$ . During this progressive examination, various topological features, such as components, loops, voids, and more, may emerge as we transition from  $Z_i$  to  $Z_j$  and subsequently disappear.

Persistent homology captures the birth and death of these topological features, quantified through homology classes. Specifically, the  $k$ -dimensional persistence diagram denoted as  $D_k$ , consists of a diagonal line and a multiset of persistence points in the "birth-death" plane. Each persistence point  $(b, d)$  records that a  $k$ -dimensional topological feature comes into existence upon entry into  $Z_b$  and dies upon entry into  $Z_d$ . The persistence of this feature is represented by its lifespan, defined as  $|d - b|$ . There are various methods to construct a filtration for a space  $Z$ , each offering distinct insights into the topological characteristics of  $Z$ . One common approach involves leveraging the superlevel-sets. First, we define the super-level set of  $Z$  with respect to  $\alpha \in \mathbb{R}$  by

$$Z_\alpha = \{z \in Z : g(z) \geq \alpha\} = g^{-1}([\alpha, \infty]).$$

where  $g : Z \rightarrow \mathbb{R}$  is a smooth function and  $\alpha$  starts at  $\infty$  and then declines towards  $-\infty$ . If  $\alpha_1 > \alpha_2$ , we have the inclusion  $Z_{\alpha_1} \subseteq Z_{\alpha_2}$ . For  $k = 1, 2, \dots$ , the  $k$ -th homology gives information about the  $k$ -dimensional holes: For  $k = 0$ , this refers to connected components; for  $k = 1$ , it refers to loops; for  $k = 2$ , it is voids, and so on. The number  $\alpha$  is called a  $p$ -critical value of  $g$  if the number of connected components of  $Z_{\alpha-\varepsilon}$  and  $Z_{\alpha+\varepsilon}$  changes for  $k = 0$ , or if the number of loops in  $Z_{\alpha-\varepsilon}$  and  $Z_{\alpha+\varepsilon}$  changes for  $k = 1$ , for all small  $\varepsilon > 0$ . Usually, the function  $g$  is a distance function or a smooth function such as the kernel density estimator. In this paper, we use the Gaussian kernel density estimator (KDE). Based on a sample  $\hat{Z}_n = \{z_i\}_{i=1}^n$  in  $Z$ , KDE is defined as

$$g_n(y) = \frac{1}{n(\sqrt{2\pi}\eta)^D} \sum_{i=1}^n \exp\left(-\frac{\|y - z_i\|^2}{2\eta^2}\right), \quad y \in \mathbb{R}^D$$

where  $\eta > 0$  is a bandwidth parameter for the Gaussian kernel defining  $g_n$ .

### Wasserstein distance between persistence diagrams

To take advantage of the topological information and topological properties derived by persistent homology, one must be able to compare persistence diagrams, i.e. endow the space of persistence diagrams with a metric structure. The similarity between the two persistence diagrams is commonly measured by the Wasserstein distance. The  $p$  Wasserstein distance<sup>22</sup> for  $p \geq 1$ , between two persistence diagrams  $D_X$  and  $D_Y$  corresponding to data sets  $X$  and  $Y$  is defined as

$$WD_p(D_X, D_Y) = \left( \inf_{\gamma} \sum_{a \in D_X} \|a - \gamma(a)\|_\infty^p \right)^{\frac{1}{p}}.$$

where  $\gamma$  ranges over all bijections from the points in  $D_X$  to the points in  $D_Y$ . One can assume that a persistence diagram is a countable multi-set of points in  $\mathbb{R}^2$  along with the diagonal where each point on the diagonal has infinite multiplicity. In this way the cardinalities of  $D_X$  and  $D_Y$  are considered to be equal. Ref. 23 provides the stability theorem for the Wasserstein distance between two persistence diagrams. They showed that the persistence diagrams of filtrations created on top of data sets turn out to be quite stable with regard to some perturbations of the data.

## GPD: The Gibbs distribution-based parametric Model for Persistence Diagrams

We use the parametric model based on Gibbs distribution for persistence diagrams (GBD)<sup>19,24</sup> to statistically validate our results. The primary motivation for selecting this model is attributed to our constrained data scenario, wherein we possess only a single sample of the agent data. This approach is specifically tailored to function effectively with a single persistence diagram, making it a suitable choice for our analysis. We provide a concise overview below.

The subsequent description outlines a procedure for a set of  $N$  points on a persistence diagram  $D_k$  for fixed homology group  $k$ . Given the set  $\mathcal{Z}_N = \{b_i, d_i\}_{i=1}^N$  of birth death pairs on the persistence diagram  $D_k$ , construct a new set  $\mathcal{X}_N = \{x_i\}_{i=1}^N$ , with  $x_i^{(1)} = d_i$  and  $x_i^{(2)} = b_i - d_i$ . That is,  $\mathcal{X}_N$  is a set of  $N$  points in  $\mathbb{R} \times \mathbb{R}_+$ . This transformation projects the diagonal line on  $D_k$  on the horizontal axis resulting in a projected persistence diagram  $PD_k$ . Let  $x_q \in \mathcal{X}_N$ , for  $q \geq 1$  denotes the  $q$ -th nearest neighbor of  $x$ , for any  $x \in \mathcal{X}_N$ . Define  $\mathbb{L}_q(\mathcal{X}_N)$  as

$$\mathbb{L}_q(\mathcal{X}_N) = \sum_{x \in \mathcal{X}_N} \|x - x_q\|.$$

The statistical model for  $PD_k$  is represented by the Gibbs distribution, given as follows:

$$\phi_{\Theta}(\mathcal{X}_N) = \frac{1}{Z_{\Theta}} \exp(-H_{\Theta}^K(\mathcal{X}_N)),$$

where  $\Theta = (\theta_0, \theta_1, \dots, \theta_K)$  and  $H_{\Theta}^K(\mathcal{X}_N) : \mathbb{R}^N \rightarrow \mathbb{R}$  is defined for  $K \geq 1$  as:

$$\tilde{H}_{\Theta}^K(\mathcal{X}_N) = \sum_{q=1}^K \theta_q \mathbb{L}_q(\mathcal{X}_N) \times (g_n(\mathcal{X}_N))^{\theta_0}.$$

Since the analytical form of  $Z_{\Theta}$  is not known, the estimation of parameters is done using the pseudo-likelihood approach<sup>19</sup>. The pseudo-likelihood function is given by

$$\mathcal{L}_{\Theta}^K(\mathcal{X}_N) = \prod_{x \in \mathcal{X}_N} f_{\Theta}(x|N_K(x))$$

where  $N_K(x)$  denotes the  $K$  nearest neighbors of  $x$  in  $\mathcal{X}_N$ , and

$$f_{\Theta}(x|N_K(x)) = \frac{\exp(-\tilde{H}_{\Theta}^K(x|N_K(x)))}{\int_{\mathbb{R}} \int_{\mathbb{R}_+} \exp(-\tilde{H}_{\Theta}^K(z|N_K(x))) dz^{(1)} dz^{(2)}}$$

with

$$\tilde{H}_{\Theta}^K(x|N_K(x)) = \sum_{q=1}^K \theta_q \mathbb{L}_k(N_K(x)) \times (g_n(x))^{\theta_0}$$

The parameter  $\theta_0$  is a non-negative parameter. Note that nearest neighbors capture the closeness relations between the points, and  $g_n$  controls the shape of the whole points on the persistence diagram. The parameter set  $\Theta$  is learned by minimizing the negative log-likelihood, which is given by

$$\begin{aligned} -\log(\mathcal{L}_{\Theta}^K(\mathcal{X}_N)) &= -\sum_{x \in \mathcal{X}_N} \log(f_{\Theta}(x|N_K(x))) \\ &= -\sum_{x \in \mathcal{X}_N} \log(\exp(-\tilde{H}_{\Theta}^K(x|N_K(x)))) + \log\left(\int_{\mathbb{R}} \int_{\mathbb{R}_+} \exp(-\tilde{H}_{\Theta}^K(z|N_K(x))) dz^{(1)} dz^{(2)}\right) \end{aligned}$$

So, the simplified negative log-likelihood is

$$\sum_{x \in \mathcal{X}_N} \tilde{H}_{\Theta}^K(x|N_K(x)) + \sum_{x \in \mathcal{X}_N} \log\left(\int_{\mathbb{R}} \int_{\mathbb{R}_+} \exp(-\tilde{H}_{\Theta}^K(z|N_K(x))) dz^{(1)} dz^{(2)}\right)$$

This parametric model allows to model  $PD_k$  obtained using a given data sample. Based on the model, we can check if two data sets come from the same distribution by fitting a model to the projected persistence diagrams of each data set and then comparing the estimates. We do this by testing the hypothesis  $H_{null} : \theta_j^1 = \theta_j^2$  vs. the alternative hypothesis  $H_{alt} : \theta_j^1 \neq \theta_j^2$ , for

$j = 0, 1, \dots, K$ , where  $\Theta_i = (\theta_1^i, \theta_2^i, \dots, \theta_n^i)$   $i \in \{1, 2\}$  are parameters for the fitted models for two data sets. The test-statistics is given by

$$T = \left| \frac{\hat{\theta}_j^1 - \hat{\theta}_j^2}{\sqrt{\text{Var}(\hat{\theta}_j^1) + \text{Var}(\hat{\theta}_j^2)}} \right| \quad (3)$$

where  $\hat{\theta}_j^s$  is the estimated  $\theta_j^s$  for  $s \in \{1, 2\}$ . Based on the asymptotic properties of the pseudo-likelihood, the p-value is obtained by

$$2 \times P \left( Z > \left| \frac{\hat{\theta}_j^1 - \hat{\theta}_j^2}{\sqrt{\text{Var}(\hat{\theta}_j^1) + \text{Var}(\hat{\theta}_j^2)}} \right| \right),$$

where  $Z$  is the standard normal random variable. The variances of the estimates are based on the empirical Fisher information matrix. In the present paper, we have chosen to set a maximum value for  $K = 3$  as prior research has demonstrated that increasing the value of  $K$  beyond 3 yields only marginal improvements<sup>19</sup>. The code for estimating the parameters of GPD is available on GitHub <https://github.com/Anubha0812/GPD>.

### Synthetic data and Monte-Carlo experiments

We conducted a Monte Carlo simulation to model the complex dynamics of social connections between agents. Synthetic data was generated using the Independent Cascade (IC) model, to rigorously test both robustness and performance of our proposed approach. Below, we detail the underlying assumptions and the procedures employed in generating the synthetic dataset:

1. **Graph Representation:** Let  $G = (V, E)$  be a directed graph where  $V$  denotes the set of nodes representing the agents, and  $E$  denotes the set of directed edges representing information links between agents. The total number of agents is represented by  $N = |V|$ .
2. **Social Network Construction:** The social network structure among agents is drawn from observed insider networks. Whenever two agents are insiders of the same company, we assume there exists a directed edge between them in both directions. We only consider the edges that connect agents to the largest component of this social graph, leaving some agents completely unconnected.
3. **Agent Classification by Information Sharing Probability:** Agents are randomly assigned to one of three classes. Each class has a different probability of sharing information, denoted by  $q_i$  for class  $i$ , where  $i \in \{1, 2, 3\}$ .
4. **Assignment of Edge Weights:** Edge weights,  $w_{ij}$ , between connected agents  $i$  and  $j$  are determined based on the class of agent  $i$  as follows: If agent  $i$  is in class 1, the edge weight is sampled from a uniform distribution  $q_1 \sim U(0, 0.2)$ . This process is iterated for each agent to assign edge weights across the entire graph.
5. **Agent Grouping and Trading Probability Modeling:** We model how agents behave if they receive information by assigning each into one of three distinct behavioral groups: Passive, Neutral, and Opportunistic agents. Each group has a different distribution for trading when they receive information. This models differences in reactivity to new information. Agents with no path to any other companies are considered unconnected and are never informed. The trading probabilities are defined as follows:

$$p_{\text{Passive}} \in (0.0, 0.4), \quad p_{\text{Neutral}} \in (0.3, 0.6), \quad p_{\text{Opportunistic}} \in (0.5, 0.8), \quad p_{\text{Uninformed}} \in (0, 0.4).$$

Returns for both informed and uninformed agents are assumed to follow a normal distribution, with a constant standard deviation  $\sigma = 0.0015$ . The mean return values are defined as  $\mu_1 = 0.003$  for informed agents, capturing their higher expected profitability, while for uninformed agents, the mean is set at either  $\mu_2 = 0.0005$ , or  $\mu_2 = 0.0015$  under alternative scenarios, highlighting the relative disadvantage of being not informed. Detailed group compositions and corresponding parameters are summarized in Table 3.

6. **Baseline Model:** The baseline model simulates agent behavior in the absence of market information, where all agents trade with a probability of  $p_{\text{Uninformed}} \in (0, 0.4)$ . Returns generated under this model are distributed according to  $\mathcal{N}(0.0005, 0.0015)$ , or alternatively,  $\mathcal{N}(0.0015, 0.0015)$ , representing the baseline distribution of uninformed trading scenarios.

**Table 3.** Edge Weights and Group Composition with Trading Probabilities and Return Distributions

% Agents in Each Group	Passive	Neutral	Opportunistic
	$p_{\text{Passive}} \in (0.0, 0.4)$	$p_{\text{Neutral}} \in (0.3, 0.6)$	$p_{\text{Opportunistic}} \in (0.5, 0.8)$
$q_1 \in (0, 0.2)$ [Class-1]	0.25	0.1	0.05
$q_2 \in (0.2, 0.4)$ [Class-2]	0.15	0.2	0.1
$q_3 \in (0.4, 0.6)$ [Class-3]	0.05	0.07	0.03
	Return Distribution	Trading Probabilities	
Informed Agents	$\mathcal{N}(0.003, 0.0015)$	Based on Agent category	
Not Informed Agents	$\mathcal{N}(0.0005, 0.0015)$ or $\mathcal{N}(0.0015, 0.0015)$	$p_{\text{Uninformed}} \in (0, 0.4)$	

7. **Independent Cascade (IC) Model:** To simulate the diffusion of information, the IC model employs a probabilistic framework to propagate information from seed nodes through the network. The following steps describe the IC model implementation:

- (a) Initialize the seed nodes as the primary sources of information.
- (b) Set the state of each node as uninformed, except for the seed nodes which are set as informed.
- (c) Mark all edges as “not yet tried,” indicating that they have not been used to transmit information.
- (d) For each iteration, identify the set of newly informed nodes, starting with the seed nodes, and attempt to inform their 1-hop neighbors:
  - i. For each informed node, evaluate its outgoing edges to 1-hop neighbors.
  - ii. Generate a random variable  $r \sim U(0, 1)$ . If the edge weight  $w_{ij}$  exceeds  $r$ , the neighboring node becomes informed, and the edge is marked as “tried.”
  - iii. Repeat this process iteratively until no new nodes can be informed.

This algorithm captures the stochastic nature of information spread within the network, allowing us to obtain the final state of each node as either informed or uninformed.

8. **Trading Decisions of Informed and Uninformed Agents:** Informed nodes utilize available information to make trading decisions, with trading probabilities contingent upon their classification. Opportunistic agents, for example, trade with a probability  $p_{\text{Opportunistic}} \in (0.5, 0.8)$ , while their returns are drawn from  $\mathcal{N}(0.003, 0.0015)$ . Uninformed nodes, by contrast, trade with a probability  $p_{\text{Uninformed}} \in (0, 0.4)$ , and their returns are governed by the baseline distribution  $\mathcal{N}(0.0005, 0.0015)$  or alternatively,  $\mathcal{N}(0.0015, 0.0015)$ .

Using this setup, we simulate 1,000 iterations for both the IC and baseline models for each seed company, producing two  $N \times 1000$  return matrices. These matrices are then concatenated to form a single  $N \times 2000$  return matrix, which serves as the input for subsequent analyses.

### Data pre-processing

We describe the various pre-processing procedures employed, which involve transforming raw data into a suitable format for further analysis. Let  $N$  and  $M$  denote the number of agents and companies, respectively.

As in ref. 14, for each agent  $i, i = 1, 2, \dots, N$  and her/his executed trade  $z$  in security  $k$ , let  $Q_{i,k,z}$  be the quantity of shares traded,  $P_{i,k,z}$  the transaction price, and  $V_{i,k,z} = Q_{i,k,z} \times P_{i,k,z}$ , the traded euro volume. To determine the profit and return from an investment made by agent  $i$ , for each transaction  $z$  we define the  $\Delta T$ -day log return as

$$r_{i,k,z}^{\Delta T} = \text{sign}(z) \times \log \left( \frac{P_{k,z}^{\Delta T}}{P_{i,k,z}} \right),$$

where for security  $k$ ,  $P_{k,z}^{\Delta T}$  is the median transaction price on a day  $\Delta T = 7$  calendar days after the transaction  $z$  was executed, and  $\text{sign}(z)$  is equal to  $-1$  if  $z$  was a sale, and  $1$  if it was a purchase transaction. Here,  $r_{i,k,z}^{\Delta T}$  captures the returns generated

within a week after a trade. In cases where the price  $P_{k,z}^{\Delta T}$  one week later is unavailable, we substitute it with the price observed on the next available trading day. The profit from the investment is then obtained by multiplying the return by the investment volume (in Euros). To calculate the realised returns for each day made by agent  $i$  in the company  $j$ , we aggregate the profits from all investments made by the agent on that day in the given company we define the value-weighted average return for the agent  $i$  in security  $k$  as

$$r_{i,k}^{\Delta} = \frac{\sum_z r_{i,k,z}^{\Delta} V_{i,k,z}}{\sum_z V_{i,k,z}}.$$

This is necessary because an agent may conduct multiple trades in a single day involving different securities or the same securities of a single company.

Next, we elaborate on the methodology for calculating realised returns and profits during the pre-announcement period. For a specific company  $j \in 1, \dots, M$  and a given time window  $\delta = (t_j - |\delta|, t_j)$ , where  $|\delta| > 0$  (for example, a week with  $|\delta| = 5$  or a month with  $|\delta| = 20$ , in this case, we consider one week), each agent  $i$  is attributed a total return and net profit, summarizing their trading activities during that period. Here,  $t_j$  denotes the announcement day when company  $j$  makes public announcements, and  $\delta$  represents the informed period, during which informed trading occurs in the securities of company  $j$ .

In scenarios where we have two announcements with overlapping periods, we handle the overlap by excluding the common period between the two announcements. For example, if an announcement is made for company  $j$  on day  $t$ , and another announcement is made on day  $t + 3$ , the informed period for the first announcement is defined as  $(t - 5, t)$ , capturing the four trading days preceding the announcement day. This period represents the timeframe during which informed trading may have occurred based on the information disclosed regarding the first announcement. Similarly, for the second announcement, the informed period is  $(t - 2, t + 3)$ , covering the four trading days before the announcement day. This period reflects the interval during which informed trading could have taken place based on the information revealed in the second announcement. To ensure independence between the informed periods of the two announcements and avoid any potential overlap, we exclude the common period  $[t - 1]$  from the second informed period. Additionally, we define the non-announcement periods for each company as the trading days that fall outside the announcement period for that company, as mentioned above. These days do not include any announcements or periods of potential informed trading.

## References

1. Gomez-Rodriguez, M., Leskovec, J. & Krause, A. Inferring networks of diffusion and influence. *ACM Transactions on Knowl. Discov. from Data (TKDD)* **5**, 1–37 (2012).
2. Newman, M. Message passing methods on complex networks. *Proc. Royal Soc. A* **479**, 20220774 (2023).
3. Pouget-Abadie, J. & Horel, T. Inferring graphs from cascades: A sparse recovery framework. In *International Conference on Machine Learning*, 977–986 (PMLR, 2015).
4. Wilinski, M. & Lokhov, A. Prediction-centric learning of independent cascade dynamics from partial observations. In *International Conference on Machine Learning*, 11182–11192 (PMLR, 2021).
5. Lokhov, A. & Wilinski, M. Learning of networked spreading models from noisy and incomplete data. *Bull. Am. Phys. Soc.* (2024).
6. European Centre for Disease Prevention and Control. Options for the use of rapid antigen tests for covid-19 in the eu/eea and the uk. Tech. Rep., ECDC (2020).
7. Singh, G., Mémoli, F., Carlsson, G. E. *et al.* Topological methods for the analysis of high dimensional data sets and 3d object recognition. *PBG@ Eurographics* **2**, 091–100 (2007).
8. Carriere, M., Michel, B. & Oudot, S. Statistical analysis and parameter selection for mapper. *J. Mach. Learn. Res.* **19**, 1–39 (2018).
9. Rahman, A. & Verma, B. Novel layered clustering-based approach for generating ensemble of classifiers. *IEEE Transactions on Neural Networks* **22**, 781–792 (2011).
10. Baltakys, K., Baltakiene, M., Heidari, N., Iosifidis, A. & Kannianen, J. Predicting the trading behavior of socially connected investors: Graph neural network approach with implications to market surveillance. *Expert. Syst. with Appl.* **228**, 120285 (2023).
11. Ozsoylev, H. N., Walden, J., Yavuz, M. D. & Bildik, R. Investor networks in the stock market. *The Rev. Financial Stud.* **27**, 1323–1366 (2014).
12. Tumminello, M., Lillo, F., Piilo, J. & Mantegna, R. N. Identification of clusters of investors from their real trading activity in a financial market. *New J. Phys.* **14**, 013041 (2012).
13. Ranganathan, S., Kivelä, M. & Kannianen, J. Dynamics of investor spanning trees around dot-com bubble. *PloS one* **13**, e0198807 (2018).
14. Baltakienė, M., Kannianen, J. & Baltakys, K. Identification of information networks in stock markets. *J. Econ. Dyn. Control.* **131**, 104217 (2021).
15. Ahern, K. R. Information networks: Evidence from illegal insider trading tips. *J. Financial Econ.* **125**, 26–47 (2017).
16. Givoly, D. & Palmon, D. Insider trading and the exploitation of inside information: Some empirical evidence. *J. business* 69–87 (1985).
17. Fidrmuc, J., Goergen, M. & Renneboog, L. Insider trading, news releases, and ownership concentration. In *Insider Trading*, 309–370 (CRC Press, 2008).
18. Lakonishok, J. & Lee, I. Are insider trades informative? *The Rev. Financial Stud.* **14**, 79–111 (2001).
19. Adler, R. J., Agami, S. & Pranav, P. Modeling and replicating statistical topology and evidence for cmb nonhomogeneity. *Proc. Natl. Acad. Sci.* **114**, 11878–11883 (2017).
20. Brown, A., Bobrowski, O., Munch, E. & Wang, B. Probabilistic convergence and stability of random mapper graphs. *J. Appl. Comput. Topol.* **5**, 99–140 (2021).
21. Fasy, B. T. *et al.* Confidence sets for persistence diagrams. *The Annals Stat.* **42** (2014).
22. Edelsbrunner, H. & Harer, J. *Computational Topology: An Introduction* (American Mathematical Soc., 2010).
23. Cohen-Steiner, D., Edelsbrunner, H., Harer, J. & Mileyko, Y. Lipschitz functions have  $l^p$ -stable persistence. *Foundations Comput. Math.* **10**, 127–139 (2010).
24. Agami, S. Improved modeling of persistence diagram. *arXiv preprint arXiv:2205.10907* (2022).
25. MacQueen, J. *et al.* Some methods for classification and analysis of multivariate observations. In *Proceedings of the fifth Berkeley symposium on mathematical statistics and probability*, vol. 1, 281–297 (Oakland, CA, USA, 1967).
26. Arthur, D., Vassilvitskii, S. *et al.* k-means++: The advantages of careful seeding. In *Soda*, vol. 7, 1027–1035 (2007).



27. Ester, M., Kriegel, H.-P., Sander, J., Xu, X. *et al.* A density-based algorithm for discovering clusters in large spatial databases with noise. In *kdd*, vol. 96, 226–231 (1996).
28. Murtagh, F. & Contreras, P. Algorithms for hierarchical clustering: an overview. *Wiley Interdiscip. Rev. Data Min. Knowl. Discov.* **2**, 86–97 (2012).
29. Chandola, V., Banerjee, A. & Kumar, V. Anomaly detection: A survey. *ACM computing surveys (CSUR)* **41**, 1–58 (2009).

## Supplementary Information

### Toy Example for Motivating the Use of Mapper over Direct Clustering Methods

To illustrate the limitations of traditional clustering methods and highlight the advantages of the Mapper algorithm, we consider a toy example involving the return profiles of three agents: Agent 1 ( $A_1$ ), Agent 2 ( $A_2$ ), and Agent 3 ( $A_3$ ). The return profiles for each agent are represented as sequences of values over time, capturing their trading behavior:

$$A_1 : [0.005, 0.005, 0, 0, 0.005, 0, 0.005],$$

$$A_2 : [0, 0, 0.005, 0.005, 0, 0.005, 0],$$

$$A_3 : [-0.005, 0, 0, 0, 0, 0, 0].$$

We compute the pairwise Euclidean distances (ED) between these agents to assess their similarity in terms of return profiles:

$$ED(A_1, A_2) = \sqrt{\sum_{t=1}^7 (A_1(t) - A_2(t))^2} = \sqrt{0.01323},$$

$$ED(A_1, A_3) = \sqrt{\sum_{t=1}^7 (A_1(t) - A_3(t))^2} = \sqrt{0.01323},$$

$$ED(A_2, A_3) = \sqrt{\sum_{t=1}^7 (A_2(t) - A_3(t))^2} = \sqrt{0.01}.$$

Traditional clustering methods such as K-means rely heavily on geometric distances like the Euclidean distance to group data points. In this example, K-means clustering would calculate the centroids and assign agents to clusters based on their proximity to these centroids. Given the computed distances,  $A_1$  is equidistant from both  $A_2$  and  $A_3$ , suggesting equal similarity to both. However, the smallest distance is observed between  $A_2$  and  $A_3$ , prompting the algorithm to group  $A_2$  and  $A_3$  into the same cluster.

From a financial perspective, this grouping is counterintuitive. Although the return sequences of  $A_2$  and  $A_3$  are numerically close, their trading behaviors suggest different underlying motivations.  $A_1$  and  $A_2$  exhibit patterns consistent with informed trading, characterized by positive returns in correlated periods, while  $A_3$  shows a distinct behavior with mostly zero returns and a negative initial value, indicative of uninformed or passive trading.

Direct clustering methods such as K-means fail to capture the nuanced trading behaviors that are crucial for identifying suspicious or informed trading. The primary limitation lies in the reliance on purely geometric distances, which do not consider the temporal sequence or contextual relevance of the trades. This approach disregards the underlying economic rationale that could better distinguish between informed and uninformed agents.

The Mapper algorithm overcomes these limitations by incorporating a topological approach that analyzes the shape of the data in a multi-dimensional feature space. Rather than clustering based solely on distance metrics, Mapper first applies a filter function to capture key aspects of the data, such as return, volatility, trading frequency, or other domain-specific metrics. This filter function transforms the data into a simplified representation that emphasizes behavioral patterns rather than raw numerical distances. In the example, the Mapper algorithm can differentiate  $A_1$  and  $A_2$  as engaging in informed trading while isolating  $A_3$  as uninformed, addressing the core limitation of K-means in this context.

It is worth highlighting that our approach effectively addresses two key challenges:

1. It enables the identification of groups of agents who exhibit suspicious trading behavior, especially during periods of new information releases.
2. The within-bin clustering process inherent to our Mapper strategy is particularly valuable, as it allows the detection of synchronized trading actions among agents within each cluster. This approach identifies groups of agents engaging in coordinated trading activities, whether profitable, unprofitable, or no-trade cases, along with the specific timing of these trades.

This dual capability of detecting both suspicious behavior and synchronization in trading provides a robust framework for analyzing agent activities, making it a powerful tool in financial market surveillance.

## Data on insider networks

In our empirical analysis, we assume that information spreads before the arrival of a public company announcement, resulting in a cascade of opportunistic trading. The hypothesis is that information may begin to spread from a company's board through social links prior to an announcement. To analyze this hypothesis, we use a unique and rich data set combined from multiple sources: (i) Data that contains the insider network in Finland: Being an insider in the same company creates a social link between all members. Overlapping board memberships thus result in a large social network; (ii) Information of board members and insiders' mandatory disclosure notifications, which allowed us to identify partial trading patterns; (iii) A unique and extensive pseudonymized dataset containing detailed trading records of all investors across all securities on the Helsinki Stock Exchange; (iv) Data related to company announcements. By integrating these datasets, we have created unique data that contains not only the social links between insiders but also track all their transactions across all securities extending beyond those restricted by insider trading regulations (see our recent paper<sup>10</sup>). To ensure compliance with relevant legislation, all personal data within the dataset is pseudonymized, we do not access any information that identifies the individuals.

Descriptive statistics for the data are presented in Table 4. The data encompasses the period from 05/2005 to 12/2009, which includes 1,159 trading days across 122 companies. We designated each trading day as occurring either inside or outside a pre-announcement period for a given company, based on whether an unscheduled announcement was made by the company within four days. There were 1,596 identified investors. We removed trades in companies that do not have any trades during pre-announcement periods. The remaining data consists of 119 companies and 1586 investors, and 1490 of the investors made at least one trade during pre-announcement periods and one outside these periods, and we labeled these as active. There were a total of 293,750 transactions, with 81,634 occurring within the pre-announcement periods. An average investor was socially connected to 17.3 other investors in the insider network. Approximately 22% of the investors were female.

There is a significant variation in the liquidity of companies: the most liquid companies are traded nearly every day by at least one investor included in our analysis, while the least liquid are traded only on a few days per year. This is mirrored in the transaction numbers for different companies, with the highest being 3,544 and the lowest around 2. On average, each company made 19 announcements per year. However, the frequency of announcements varied significantly, with some companies having as few as 2 announcements per year, while others had as many as 69 announcements annually. For an average investor, around 23% of transactions were located within the pre-announcement periods. 24.49% of their profitable and 22.02% unprofitable transactions were located within the pre-announcement periods. Out of an average of 669 transactions, 339 were profitable, which is very close to 50%. The table also shows the age distribution.

The first two plots from the left-hand side in Figure 1(a) show how companies are distributed with respect to the total number of transactions executed by all investors and with respect to the percentage of pre-announcement trades. Due to variations in the number of announcements across different companies, the number of pre-announcement days also varies for each company. We find that a majority of the companies were quite illiquid in terms of the number of transactions, and for most companies, the pre-announcement days constituted about 20-40% of all trading days.

To gauge the robustness of our analysis, we conduct additional assessments by filtering companies based on transaction volume. We present results for the top 24, 18, and 11 liquid companies, using a cut-off of a minimum of 5,000, 6,000, and 7,000 total transactions, respectively. It is noteworthy that, in the case of all companies, the least liquid company had 59 transactions in total.

## Method Validation using Monte Carlo Experiments

### Data generation

To validate the methods in our framework, we created synthetic data that establishes a ground truth for the status of each agent. This ground truth serves solely for validation purposes; the identification of agent status is conducted in an unsupervised manner using the method described in the Method section. Our Monte Carlo experiments utilize a graph that represents an actual insider network, within which we simulate random information cascades, using the independent cascade model.

To make the Monte Carlo experiment as realistic as possible, an actual insider network (see Section Dataset) is used to construct a graph  $G = (V, E)$ , where  $V$  represents the set of agents, and  $E$  denotes the set of edges, representing social connections. A social connection is assumed to exist if two agents are insiders in the same company. We only consider the largest connected component gained this way, and only the corresponding companies are simulated. We use a larger dataset for the synthetic validation. In our dataset, there are a total of 1830 agents, of which 1596 have some transactions. 127 of these agents have no connections to the largest component of the graph, and are totally isolated; They serve as "sure false positives", i.e., they never have access to inside information.

The remaining agents are divided into three randomized groups. Each group is given a probability of trading if they are informed (see Supplementary information for details). *Opportunistic agents* are given a high probability of acting upon the information, i.e., making a profitable trade. *Neutral agents* are given a moderate probability, while *passive agents* are those with a low probability of doing so. The agents who are not linked to the companies in the main component are designated

Descriptive Statistics							
Number of trading days	1,159						
Number of trading days per year	251						
Number of companies	122						
Number of investors	1,596						
Total number of transactions	293,750						
Total transactions within pre-announcement periods	81,634						
Average Degree	17.3						
Fraction of Female Investors	21.65%						
Company specific statistics	Min.	1st Qu.	Median	Mean	3rd Qu.	Max.	Std Dev
Number of trading days with transactions/company/year	0.87	30.13	56.69	72.38	105.69	226.53	56.12
Number of transactions/company/year	2.38	88.33	209.22	520.95	707.07	3544.63	686.66
Number of announcements/company/year	1.95	12.82	17.53	19.24	23.48	69.45	9.89
Investor specific statistics	Min.	1st Qu.	Median	Mean	3rd Qu.	Max.	Std Dev
Investor's unique trading days	1	3	10	30.51	27.25	654	60.64
Number of investors traded/company/year	0.6	12	20.10	44.27	56.85	268.2	51.79
Investor's all transactions/company	11.00	408.25	967.00	2407.79	3268.00	16383.00	3173.69
Investor's all transactions/company within pre-announcement periods	0.00	69.50	192.00	669.13	936.00	3839.00	948.89
Percentage of transactions within pre-announcement periods per company	0.00%	15.57%	22.14%	23.14%	29.32%	60.53%	11.24%
Investor's all profitable transactions per company	1.00	163.25	452.50	1188.47	1808.50	8517.00	1590.88
Investor's profitable transactions per company within pre-announcement periods	0.00	33.00	92.50	339.33	479.25	2271.00	490.09
Percentage of profitable transactions within pre-announcement periods per company	0.00%	15.82%	23.97%	24.49%	31.56%	68.75%	12.75%
Age Group	< 30	31-40	41-50	51-60	> 61		
	3.49%	9.00%	32.02%	26.63%	15.35%		

**Table 4.** Descriptive statistics of the empirical data.

as *unconnected agents*. The aim is to effectively filter out agents who have received insider information and acted on it. We simulate the investors' transactions and their profitability for the two periods i.e. the pre-announcement periods and non-announcement periods, using the Independent Cascade Model (see Methods for simulation setup). We perform 1,000 simulations each for announcement and non-announcement periods for each of the companies as seed companies.

In each cascade, the information spreading starts from the seed company and spreads across the network based on each agent's probability of sharing information. Once informed, an agent then trades based on their designated probability of acting on the information. If they trade, the return distribution follows Gaussian  $\mathcal{N}(0.003, 0.0015)$ . Uninformed agents, regardless of their classification, trade according to a baseline model where no information prevails in the market. A trade is accompanied by the return sampled from  $\mathcal{N}(\mu, 0.0015)$ . We consider two alternative values for  $\mu$ :  $\mu = 0.0005$  and  $\mu = 0.0015$  for the baseline model as a robustness check. Note that the unconnected agents always follow the baseline trading model as information never reaches them.

### Methods for comparative analysis

In evaluating the effectiveness of our proposed strategy, we undertake a comparative analysis with two distinct categories of models: hard clustering techniques<sup>2</sup> and unsupervised anomaly detection methods. The rationale behind this comparative approach is twofold: firstly, Mapper operates as a soft clustering technique, and we aim to gauge its performance against conventional hard clustering methods where we incorporate expert knowledge to identify the cluster corresponding to opportunistic agents. We use features extracted using the same filter functions as in the Mapper approach and compare the most commonly used clustering methods. This includes K-means<sup>25</sup>, K-means++<sup>26</sup>, Density-Based Spatial Clustering Application with Noise (DBSCAN)<sup>27</sup>, and Hierarchical Clustering (Hclust)<sup>28</sup>.

The exploitation of private information can be thought of as an anomaly in trading patterns. This is why we also check how the Mapper strategy performs relative to commonly used unsupervised anomaly detection methods that do not incorporate

<sup>2</sup>To further justify the appropriateness of Mapper over hard clustering algorithms, a toy example is given in Supplementary Information as an illustration.

expert knowledge. We use the One-Class Support Vector Machine (OCSVM), K-Nearest Neighbor (KNN), Isolation Forest (IForest), and Local Outlier Factor (LOF)<sup>29</sup> methods for comparison. We set the number of bins to  $|I| = 3$ , the percentage overlap  $p = 25\%$  and employ K-means clustering with 150 clusters with Euclidean distance as the measure of dissimilarity. The specific details of the parameters for methods used for comparison are given in the Supplementary Information.

### Results of the Monte Carlo Experiments

Table 5 reports the results of the Monte-Carlo experiments. It presents how accurately the opportunistic agents were identified with the proposed Mapper-based and benchmark methods. The results are based on two different baseline distributions for uninformed investors:  $\mu = 0.0005$  and  $\mu = 0.0015$  (see Section Data Generation). The results show that when employing the Mapper algorithm, its ability to accurately identify members of opportunistic traders while minimizing false positives stands out, with a significant advantage over the other clustering methods. The Mapper strategy is more cautious in labeling agents as opportunistic, which is often desirable in real-world applications where we aim to avoid falsely labeling passive individuals. We also report the F1-scores, which give equal weight to both precision and recall. However, depending on the context, different weightings can be applied to emphasize either precision or recall as needed.

In the context of hard clustering, one might initially anticipate the formation of distinct clusters based on the three predefined groups. However, the obtained results are rather surprising. In the case of K-means, K-means++, and hierarchical clustering (Hclust), the selected clusters encompass members from all three groups, including agents who were never exposed to insider information. This observation highlights the unreliability of these methods. DBSCAN does demonstrate a marked advantage compared to the other techniques. However, it struggles to effectively differentiate between neutral and opportunistic agents.

**Table 5.** Performance of different models in identifying opportunistic agents under two different baseline model distributions,  $\mu = 0.0005$  and  $\mu = 0.0015$ . Out of the 1830 total agents, 308 were made opportunistic. The table presents the predicted positives, actual true positives (TP), false positives (FP), true negatives (TN), false negatives (FN), precision, recall, and F1-score for each model.

Model	Predicted Positive	TP	FP	TN	FN	Precision	Recall	F1-score
<b>Panel A: <math>\mu = 0.0005</math></b>								
Mapper strategy	212	208	4	1518	100	<b>0.9811</b>	0.6753	<b>0.7994</b>
K-means	998	242	756	766	66	0.2425	0.7857	0.3703
K-means++	1016	248	768	754	60	0.2441	0.8052	0.3752
Hclust	1042	251	791	731	57	0.2409	<b>0.8149</b>	0.3735
DBSCAN	360	206	154	1368	102	0.5722	0.6688	0.6177
OCSVM	795	110	685	837	198	0.1382	0.3571	0.1987
KNN	604	220	384	1138	88	0.3642	0.7143	0.4837
LOF	1440	219	1221	301	89	0.1521	0.7110	0.2487
IForest	695	224	471	1051	84	0.3223	0.7273	0.4474
<b>Panel B: <math>\mu = 0.0015</math></b>								
Mapper strategy	204	199	5	1517	109	<b>0.9755</b>	0.6468	<b>0.7771</b>
K-means	1022	245	777	745	63	0.2397	0.7955	0.3684
K-means++	1025	246	779	743	62	0.2405	0.7987	0.3696
Hclust	1056	248	808	714	60	0.2348	0.8052	0.3630
DBSCAN	413	211	202	1320	97	0.5116	0.6851	0.5864
OCSVM	1775	261	1514	8	47	0.1470	<b>0.8474</b>	0.2513
KNN	578	216	362	1160	92	0.3737	0.7013	0.4873
LOF	1283	225	1058	464	83	0.1753	0.7305	0.2837
IForest	608	158	450	1072	150	0.2599	0.5129	0.3448

As we increase the parameter  $\mu$  for the baseline model distribution, making it more aligned with the behavior of informed investors, we observe a nuanced shift in the performance of different models. The Mapper strategy, which initially exhibited a strong F1-score of 0.80 at  $\mu = 0.0005$ , shows a slight decrease to 0.78 at  $\mu = 0.0015$ . This minor decline suggests that while the Mapper strategy remains robust, the challenge of distinguishing between informed and uninformed agents becomes more pronounced as their return distributions converge. Mapper maintains high precision (around 0.98) across both scenarios, indicating its reliability in minimizing false positives even when it correctly identifies fewer true positives due to the increased

similarity in behavior. DBSCAN, which initially had a relatively high F1-score of 0.62, experiences a slightly larger drop to 0.59 as  $\mu$  increases. This is due to a rise in false positives from 154 to 202, highlighting its vulnerability to misclassifying passive agents as opportunistic ones when the baseline profit increases. We also notice that traditional clustering methods like K-means and K-means++ struggle significantly with consistently low F1-scores around 0.37, regardless of  $\mu$ . Their high false positive rates and low precision suggest they are not well-suited for scenarios where informed and uninformed behaviors are closely matched.

Overall, while the Mapper strategy performance slightly declines, it remains preferable due to its ability to maintain a balance between precision and recall. This conservative approach aligns well with the objective of accurately identifying opportunistic trading while avoiding excessive misclassification. In contrast, models like DBSCAN and traditional clustering methods may require careful calibration or additional constraints to improve their effectiveness in similar contexts.

## Methods Used for Comparison and Parameter Setting

We employed four well-established hard clustering methods to compare the performance of our proposed strategy: K-means, K-means++, Density-Based Spatial Clustering Application with Noise (DBSCAN), and Hierarchical Clustering (Hclust). To ensure a rigorous and unbiased comparison, a uniform post-clustering approach was adopted, whereby clusters were selected based on the weighted mean of standardized filter function values. Specifically, each filter function value was standardized using Z-score scaling, and a weighted average was computed with equal weights of 0.5 for each function value. This approach mitigates the influence of any single feature dominating the clustering outcome, thereby promoting a balanced assessment.

The number of clusters was set to three, aligning with our classification of agents into three distinct groups. For the Mapper strategy, a similar rationale guided our selection of three bins. The cluster with the highest mean weighted average value was designated as the group containing potentially Opportunistic agents. This methodological consistency across soft and hard clustering techniques enables a direct and unbiased evaluation of their efficacy in extracting meaningful clusters.

## Parameter Tuning for Clustering Methods

- **DBSCAN:** We experimented by varying the minimum number of points (MinPts), in the range [30,50], and varied the epsilon ( $\epsilon$ ) parameter within the range [0.05, 1.5]. After extensive testing, the optimal configuration was determined to be MinPts = 30 and  $\epsilon = 0.08$ , which yielded the best results in terms of average silhouette scores.
- **Hierarchical Clustering:** We employed Ward's method for linkage, which minimizes the variance within clusters. The hierarchical tree was subsequently segmented into three groups to maintain alignment with the classification structure used in other methods.
- **One-Class SVM:** The One-Class Support Vector Machine model was exclusively trained on data from non-announcement periods to establish a baseline representation of normal behavior. Among the four tested kernels—sigmoid, polynomial, linear, and radial—the sigmoid kernel demonstrated superior performance with the lowest rate of false positives, making it the most reliable choice for detecting deviations indicative of suspicious trading activity.
- **KNN, LOF, and Random Forest:** Anomaly scores were assigned to each data point within our dataset based on these methods. Agents with anomaly scores exceeding the 88th percentile were flagged as Opportunistic agents, consistent with our Mapper strategy, which effectively identified 208 (18%) agents within the Opportunistic group.

## True Distribution of identified opportunistic agents on the simulated data by Mapper, hard clustering, and anomaly detection methods.

Table 6 presents the actual distribution of agents identified as opportunistic, across the three categories considered. We note that as we increase the parameter  $\mu$  for the baseline model distribution, making it closer to the behavior of informed agents, there is a corresponding minor decrease in the performance of the Mapper strategy. This outcome is intuitive, as it becomes challenging to distinguish between informed and uninformed agents when the distributions of their returns become more similar. Additionally, the second-best performing model, DBSCAN, identified two passive agents as opportunistic when  $\mu$  was increased. The number of false positives remained almost constant, while only the number of true positives decreased in the case of the Mapper strategy. This comports with our original intention of exercising caution in identifying opportunistic agents. With DBSCAN, we noticed a significant rise in false positives alongside a minor increase in true positives as we increased the  $\mu$  parameter. This suggests that DBSCAN is less robust in terms of avoiding false positives. The Mapper strategy offers flexibility, as it allows for a straightforward analysis of the agents excluded in Step 3. Instead of removing these linked clusters, they can be considered for inclusion and further exploration, offering a more permissive and less conservative approach if desired.

Panel A: Baseline distribution for non-informed agents with  $\mu = 0.0005$

<b>Groups of agents with different probability levels to use inside information</b>	Total Identified	<i>Opportunistic</i> High probability	<i>Neutral</i> Moderate probability	<i>Passive</i> Low probability	<i>Unconnected</i> Zero probability
Mapper strategy	212	208	4	0	0
K-means	998	242	461	294	1
K-means++	1016	248	470	297	1
Hclust	1042	251	483	304	4
DBSCAN	360	206	154	0	0
OCSVM	795	110	225	333	127
KNN	604	220	208	176	0
LOF	1440	219	582	512	127
IForest	695	224	248	221	2

Panel B: Baseline distribution for non-informed agents with  $\mu = 0.0015$

<b>Groups of agents with different probability levels to use inside information</b>	Total Identified	<i>Opportunistic</i> High probability	<i>Neutral</i> Moderate probability	<i>Passive</i> Low probability	<i>Unconnected</i> Zero probability
Mapper strategy	204	199	5	0	0
K-means	1022	245	478	299	0
K-means++	1025	246	478	301	0
Hclust	1056	248	491	317	0
DBSCAN	413	211	200	2	0
OCSVM	1775	261	618	769	127
KNN	578	216	215	147	0
LOF	1283	225	419	512	127
IForest	608	158	256	188	6

**Table 6.** The table presents the total number of opportunistic agents identified by the Mapper strategy, Hard Clustering, and Unsupervised Anomaly Detection methods under two different baseline model distributions,  $\mu$ . Out of the 1830 total modeled agents, 308 were designated opportunistic, 626 neutral, and 769 as passive. 127 are unconnected to any seeds. The table also illustrates the actual nature of the agents identified as opportunistic by each method

### 0.1 Attributes of agents

Table 7 lists the percentage of agents that were classified as opportunistic according to region, age group, gender, and experience level. Table 8 presets how opportunistic and non-opportunistic agents were distributed according to different regions, age groups, and experience range. We see from Table 7, the highest proportion of opportunistic agents is found in Central Finland (31.82%) and Eastern Finland (23.81%), with a noticeable presence in Helsinki (17.08%). When considering age groups, the data reveals that opportunistic agents are more common in the age group 61 and above (23.14%), suggesting that older investors are more inclined towards opportunistic investment strategies. Gender distribution shows a males (15.43%) are slightly more likely to be classified as opportunistic than females (11.94%). Additionally agents with 4+ years of experience are most likely (26.12%) to be classified as opportunistic.

From Table 8 shows that most of the agents, 69.04% of opportunistic and 65.87% of others, are from Helsinki region. This is not surprising given the importance of the capital region. The distribution over the other regions reflects mostly the economic importance of the said regions. In terms of distribution by age, the largest group of agents is the age group 41–50, but only in the 61+ age group do we see a marked overrepresentation of opportunistic investors. When looked at the experience range, the contrast becomes even starker.

Together, these findings underscore the importance of investor experience and regional factors in shaping investment strategies. In particular, the prevalence of opportunistic behavior in regions like Helsinki suggests that access to markets, financial resources, and information may play a significant role. Central Finland seems anomalous in this sense, as it has a markedly higher percentage of opportunistic agents compared with others. The data indicates that older, more experienced investors tend to adopt opportunistic strategies more frequently, reinforcing the influence of accumulated market knowledge and experience on investment decisions. Additionally, the gender imbalance observed in both categories highlights a potential

**Table 7.** Percentage of agents classified as opportunistic across different regions, age groups, gender, and experience levels

Metric	Opportunistic
<b>Region Counts</b>	
Central-Finland	31.82%
Eastern-Finland	23.81%
Eastern-Tavastia	16.00%
Helsinki	17.08%
Northern-Finland	15.15%
Northern-Savonia	10.00%
Ostrobothnia	14.08%
Rest-Uusimaa	14.12%
South-East	15.79%
South-West	16.04%
Western-Tavastia	10.34%
<b>Age Counts</b>	
<30	9.09%
31-40	14.18%
41-50	14.51%
51-60	11.72%
61 and above	23.14%
<b>Gender Counts</b>	
Number of Males	15.43%
Number of Females	11.94%
<b>Experience Range</b>	
0-1 year	3.66%
1-2 years	4.46%
2-3 years	5.45%
3-4 years	7.34%
4+ years	26.12%

**Table 8.** Distribution of agents classified as opportunistic and non-opportunistic according to region, age group, gender, and experience level

Metric	Opportunistic	Others
<b>Region Counts</b>		
Central-Finland	2.93%	1.23%
Eastern-Finland	2.09%	1.32%
Eastern-Tavastia	1.67%	1.73%
Helsinki	69.04%	65.87%
Northern-Finland	2.09%	2.30%
Northern-Savonia	0.84%	1.48%
Ostrobothnia	4.18%	5.02%
Rest-Uusimaa	5.02%	6.00%
South-East	1.26%	1.32%
South-West	7.11%	7.32%
Western-Tavastia	3.77%	6.41%
<b>Age Counts</b>		
<30	2.46%	4.33%
31-40	9.85%	10.47%
41-50	35.96%	37.20%
51-60	24.14%	31.92%
61 and above	27.59%	16.09%
<b>Gender Counts</b>		
Number of Males	82.38%	77.64%
Number of Females	17.62%	22.36%
<b>Experience Range</b>		
0-1 year	1.18%	6.00%
1-2 years	2.75%	11.39%
2-3 years	4.31%	14.50%
3-4 years	9.41%	23.01%
4+ years	82.35%	45.10%

area for further exploration regarding the role of gender in investment decision-making.